

Spin and valley ordering of fractional quantum Hall states in monolayer graphene

Ngoc Duc Le and Thierry Jolicoeur

Université Paris-Saclay, CNRS, CEA, Institut de Physique Théorique, France

(Dated: November 30th, 2020)

We study spin and valley ordering in the quantum Hall fractions in monolayer graphene at Landau level filling factors $\nu_G = -2 + n/3$ ($n = 2, 4, 5$). We use exact diagonalizations on the spherical as well as toroidal geometry by taking into account the effect of realistic anisotropies that break the spin/valley symmetry of the pure Coulomb interaction. We also use a variational method based on eigenstates of the fully $SU(4)$ symmetric limit. For all the fractions we study there are two-component states for which the competing phases are generalizations of those occurring at neutrality $\nu_G = 0$. They are ferromagnetic, antiferromagnetic, charge-density wave and Kékulé phases, depending on the values of Ising or XY anisotropies in valley space. The varying spin-valley content of the states leads to ground state quantum numbers that are different from the $\nu_G = 0$ case. For filling factor $\nu_G = -2 + 5/3$ there is a parent state in the $SU(4)$ limit which has a flavor content $(1, 1/3, 1/3, 0)$ where the two components that are one-third filled form a two-component singlet. The addition of anisotropies leads to the formation of new states that have no counterpart at $\nu_G = 0$. While some of them are predicted by the variational approach, we find notably that negative Ising-like valley anisotropy leads to the formation of a state which is a singlet in both spin and valley space and lies beyond the reach of the variational method. Also fully spin polarized two-component states at $\nu = -2 + 4/3$ and $\nu = -2 + 5/3$ display an emergent $SU(2)$ valley symmetry because they do not feel point-contact anisotropies. We discuss implications for current experiments concerning possible spin transitions.

I. INTRODUCTION

The fractional quantum Hall effect¹ (FQHE) occurs in two-dimensional electron systems in a strong perpendicular field and is characterized notably by a gap for all charged excitations at some fractional filling ν of the Landau levels. Such gaps are due to electron-electron Coulomb interactions. In this regime there are excitations with fractional charges and also statistics, Abelian or even non-Abelian in some cases. There are possible opportunities for fabrication of new electronic devices using the non-Abelian statistics for quantum computation² or the interlayer phase coherence that occurs in bilayer systems for dissipationless devices³.

For many years after its discovery the FQHE has been studied almost only in the special two-dimensional electron gases formed in GaAs/GaAlAs heterojunctions. In this set-up the electron Landé g -factor and the dielectric constant of the host material conspire to reduce the Zeeman energy with respect to the Coulomb energy scale. As a consequence the spin degree of freedom in the lowest Landau level cannot be considered as frozen by the external magnetic field and FQHE ground states as well as their excited states are not always fully spin-polarized. This leads notably to quasiparticles that have nontrivial spin textures called skyrmions^{4,5}. The study of electron gases in materials such as AlAs⁶ added an extra degeneracy due to the relevance of several valleys for the electronic states.

The discovery of monolayer graphene has opened an even richer arena^{7–23} for the FQHE since there is also an additional two-fold valley degeneracy that comes to play. The central $N = 0$ Landau level of monolayer graphene is approximately fourfold degenerate because of spin and valley degrees of freedom and is partially filled for a range of filling factor $-2 \leq \nu_G \leq +2$. Integer quantum Hall states²⁴ also appear at fillings $\nu_G = 0, \pm 1$ and this is an instance of quantum Hall ferromagnetism : Coulomb interactions lead to gap opening also at these integer filling factors.

At neutrality $\nu_G = 0$ theory predicts^{25,26} competing phases with various patterns of spin and valley ordering. One can have ferromagnetic, antiferromagnetic, Kékulé or charge-density wave states. While these states are degenerate if one makes the approximation of full $SU(4)$ symmetry in spin/valley space, anisotropies will select one of these states in real samples. Changing parameters like the ratio of Zeeman energy to Coulomb energy can induce transitions between such ground states. An appealing scenario has been presented to explain a transition from an insulator to a quantum spin Hall state as the transition between the canted antiferromagnetic state and the ferromagnetic state. When the central Landau level is partially filled we expect formation of FQHE states and they will have also some pattern of spin and valley ordering. The fully $SU(4)$ symmetric case has been explored in many works^{27–36}. Inclusion of anisotropies has been studied by Abanin et al.³⁷ at the level of wavefunctions and an extension of Hartree-Fock theory has been also proposed by Sodemann and MacDonald³⁸. While the results of mean-field theory have been confirmed by exact diagonalizations³⁹ for $\nu_G = 0$ this has not been checked for the fractional quantum Hall states.

In this paper we introduce a set of variational wavefunctions constructed out of exact eigenstates of the $SU(4)$ symmetric limit. The wavefunctions are dressed by a spin and flavor configuration who is determined by minimizing the energy. The anisotropy energy can be expressed solely in terms of the pair correlation function of the parent

symmetric state. This approach generalizes the mean-field treatment of quantum Hall ferromagnetism. Within this framework we obtain the phase diagrams for the fractions $\nu_G = -2 + n/3$ ($n = 2, 4, 5$). We also perform extensive exact diagonalizations in the spherical^{40,41} and torus geometry to check the validity of the variational approach. For fractions $\nu_G = -2 + n/3$ ($n = 2, 4, 5$) there are two competing ground states in the $SU(4)$ limit. At $\nu_G = -2 + 2/3$ we have the fully polarized particle-hole partner of the $\nu_G = -2 + 1/3$ as well as a singlet state with two-component structure, well known from previous studies⁴². At $\nu_G = -2 + 4/3$ the competing states are the two-component particle-hole partner of the singlet with spin-valley content $(2/3, 2/3, 0, 0)$ and a state with a filled shell by addition to the $\nu = 1/3$ Coulomb ground state with spin-valley content $(1, 1/3, 0, 0)$. At $\nu_G = -2 + 5/3$ we have a two-component state $(1, 2/3, 0, 0)$ where the $2/3$ state is the fully polarized state and there is also a three-component state $(1, 1/3, 1/3)$ that is built from a filled Landau level plus a spin-singlet $2/3$ state as pointed out by Sodemann and MacDonald³⁸. The phase diagrams from the variational method are in agreement with the diagonalization results except for the fraction $\nu_G = -2 + 5/3$ where a large portion of the phase space is occupied by a correlated singlet state that cannot be reproduced by our set of wavefunctions. To clarify its structure we compute the pair correlation function for all combinations of spin/valley indices and find that there is an enhanced probability for pair formation of opposite spin. We discuss possible ways of favoring this new phase in real samples of graphene. While the regions of stability of the different patterns in spin and valley configurations are correctly predicted variationally the quantum numbers are different in several important cases involving antiferromagnetism. Also we observe that fully polarized phases for the states $(1, 1/3, 0, 0)$ and $(1, 2/3, 0, 0)$ still form $SU(2)$ valley multiplets even though the Hamiltonian does not have such a symmetry. This is due to the special point-contact form of the anisotropies. For all the fractions we have studied there are in general spin transitions when one varies the magnetic field. Multicomponent states are preferred at small Zeeman energies.

In section II we describe the Landau levels of monolayer graphene. In section III we introduce the Coulomb interactions and anisotropies that govern the spin/valley ordering of quantum Hall states. Section IV contains a discussion of the $SU(4)$ representations that we use in our exact diagonalization studies as well as the formulation of trial wavefunctions for fractional states with various spin/valley configurations. Section V discuss the integer quantum Hall states at $\nu_G = 0, \pm 1$. Section VI give results for fractions $\nu_G < -1$. In section VII we give evidence for similar physics at $\nu_G = -2 + 4/3$ and $\nu_G = 0$. The phases for the three-component state at $\nu_G = -2 + 5/3$ are discussed in section VIII. We give a simplified treatment of spin transitions in section IX and section X contains our conclusions.

II. GRAPHENE LANDAU LEVELS

Monolayer graphene has a simple hexagonal lattice structure that leads to a massless Dirac fermion spectrum close to the neutrality point. When applying a perpendicular magnetic field there is formation of relativistic Landau levels with energies :

$$E_N = \text{sign}(N) \frac{\hbar v_F}{\ell} \sqrt{2|N|} + \frac{1}{2} g \mu_B B \sigma, \quad N = 0, \pm 1, \pm 2, \dots \quad (1)$$

where $\ell = \sqrt{\hbar/eB}$ is the magnetic length, v_F is the velocity of the relativistic Dirac fermions, g is the Landé factor which is equal to 2 because spin-orbit coupling is negligible in graphene, μ_B is the Bohr magneton and $\sigma = \pm 1$ the spin projection onto the magnetic field direction. All these Landau levels are twice degenerate due to the presence of two valleys K and K' in the graphene Brillouin zone. In this paper we concentrate on the physics that takes place in the zero-energy $N = 0$ central Landau level for fractional filling factors. The $N = 0$ Landau level wavefunctions have the same spatial dependence as the non-relativistic two-dimensional electrons. For the $N = 0$ manifold of Landau states the valley index translates exactly into a sublattice index i.e. a valley K Landau state has nonzero amplitude only on one sublattice A while the other valley K' is entirely concentrated on the other sublattice B . An important consequence is that a sublattice potential difference Δ_{AB} is equivalent to a Zeeman field acting on the valley degree of freedom i.e. lifting the degeneracy between the valley degrees of freedom. Such a potential is not expected for suspended graphene samples but is induced notably by a hexagonal boron nitride (hBN) substrate when it is geometrically aligned with the graphene layer.

The energy levels from Eq.(1) lead to integer quantum Hall effects at graphene filling factors $\nu_G = \pm 2, \pm 6, \pm 10, \dots$. However even in the integer quantum Hall regime it was discovered that there are also states for $\nu_G = 0, \pm 1$ within the $N = 0$ Landau level. These are instances of the general phenomenon of quantum Hall ferromagnetism²⁴. Indeed the general arguments for appearance of quantum Hall ferromagnetism carry out in the case of graphene. We discuss the case of fillings $\nu_G = 0, \pm 1$ below. It is convenient to redefine the filling factor by writing $\nu = 2 + \nu_G$ so that the $N = 0$ LL now spans the range $0 \leq \nu \leq +4$. The global particle-hole symmetry maps the filling factor $4 - \nu$ onto ν so that it is enough to restrict our study to the range $0 \leq \nu \leq +2$.

III. INTERACTIONS AND ANISOTROPIES IN MONOLAYER GRAPHENE

We now discuss the effective electron-electron interactions within the $N = 0$ Landau level of monolayer graphene. The Coulomb interaction is $SU(4)$ symmetric to an excellent approximation. It leads to an energy scale which is constructed out of the magnetic length $E_C = e^2/(\epsilon\ell)$ where $\ell = \sqrt{\hbar/(eB)}$ and ϵ the dielectric permittivity of the system. The unitary $SU(4)$ symmetry mixing spin and valley degrees of freedom is however reduced by several phenomena. It has been proposed to encapsulate these splittings into the following Hamiltonian^{26,43} acting only onto the valley degrees of freedom :

$$\mathcal{H}_{aniso} = \sum_{i < j} [g_{\perp}(\tau_i^x \tau_j^x + \tau_i^y \tau_j^y) + g_z \tau_i^z \tau_j^z] \delta^{(2)}(\mathbf{r}_i - \mathbf{r}_j), \quad (2)$$

where the τ_i^{α} Pauli matrices operate only in valley space. We note that this form of the interaction is local in real space so it is not felt by quantum states that vanish when two particles coincide in space. This is the case notably for the $\nu = 1/3$ Laughlin wavefunction. This simple model reminiscent of the XXZ model for magnetic systems has several desirable features, notably it describes the metal-insulator transition observed at $\nu = 0$ when tilting the magnetic field away from the direction perpendicular to the sample as we discuss below¹⁵. It is convenient to parameterize the two coefficients $g_{\perp, z}$ with an angular variable θ :

$$g_{\perp} = g \cos \theta, \quad g_z = g \sin \theta, \quad (3)$$

in addition to an overall strength g which we take as positive. It is convenient to convert the parameters $g_{\perp, z}$ into two separate energy scales :

$$u_{\perp} = \frac{g_{\perp}}{2\pi\ell_B^2}, \quad u_z = \frac{g_z}{2\pi\ell_B^2}. \quad (4)$$

One can define dimensionless strengths of anisotropies by factoring out the Coulomb energy scale :

$$\tilde{g} = (g/\ell_B^2)/(e^2/(\epsilon\ell_B)) \quad (5)$$

One-body energy level splitting occurs through the Zeeman effect that acts on the spins and sublattice splitting onto the valley indices :

$$\mathcal{H}_{1body} = -\epsilon_Z \sum_i S_i^z + \Delta_{AB} \sum_i T_i^z. \quad (6)$$

The Zeeman energy ϵ_Z is $g\mu_B B_T$ where B_T is the total field and the Landé factor $g = 2$ since spin-orbit coupling is negligible in graphene. We note that the direction of the field is arbitrary due to spin rotation invariance. On the contrary the sublattice symmetry breaking takes place between the two valleys. In the case of the commonly used hBN substrate typical values of the splitting Δ_{AB} are of the order of 10 meV and are magnetic field independent.

The special Hamiltonian Eq.(2) has some symmetry properties that are independent of the filling factor. There are symmetries like those of the XXZ Heisenberg Hamiltonian well known in the field of quantum magnetism. Notably one can always perform rotations in valley space around the z axis. These form a $U(1)$ symmetry group leading to the conservation of T_z , the projection of the isospin onto the z axis. When $u_z = u_{\perp}$ ($\theta = \pi/4, \pi + \pi/4$) there is invariance under full rotation in valley space with a group $SU(2)$. Beyond these obvious symmetries, we note that for $u_{\perp} = 0$ ($\theta = \pi/2, 3\pi/2$) one can make spin rotations independently in each valley so there is a symmetry $SU(2)_K \times SU(2)_{K'}$. There is also an additional $SO(5)$ symmetry when $u_z + u_{\perp} = 0$ ($\theta = 3\pi/4, 7\pi/4$) which is not obvious in the present formulation⁴⁴.

It is important to keep in mind that the anisotropic Hamiltonian Eq.(2) has no fundamental significance. It should be viewed as the most relevant perturbation beyond the $SU(4)$ symmetric Coulomb interaction. In the real world there will be weaker anisotropic interactions between electrons with non-zero relative angular momentum. We also note that the magnitude of the couplings g_z, g_{\perp} is still uncertain. Constraints on their values come from the metal-insulator transition in tilted field observed at neutrality¹¹.

IV. INTEGER FILLINGS $\nu_G = 0, \pm 1$

If we consider the integer quantum Hall state at $\nu = 1$ then there is a set of exact eigenstates of the Coulomb problem with a closed form given by a single Slater determinant :

$$|\Psi_{\nu=1}\rangle = \prod_m c_{m\alpha}^{\dagger} |0\rangle, \quad (7)$$

where $|\alpha\rangle$ is an arbitrary four component vector in spin-valley space. The integer m is the index of the orbital Landau level and the product runs over all values of m , corresponding to complete filling of the level. This state is an exact eigenstate provided one neglects Landau level mixing. This fact is aptly called quantum Hall ferromagnetism²⁴. The arbitrariness in the direction of $|\alpha\rangle$ is fixed presumably by lattice effects beyond the simple continuum models we consider⁴³. Notably such a wavefunction Eq.(7) vanishes when electrons coincide in real space and so it is insensitive to perturbations like the anisotropies of Eq.(2).

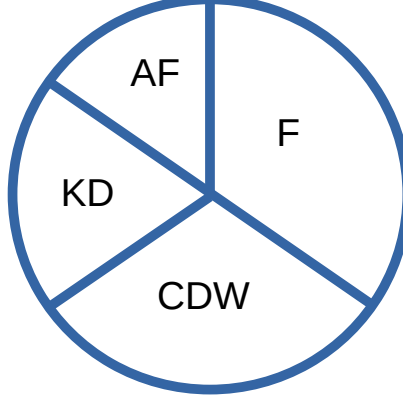


FIG. 1: Phase diagram for neutrality $\nu = 2$. The various ground states are displayed as a function of the anisotropy angle θ that varies $g_z = g \sin \theta$ and $g_\perp = g \cos \theta$. For small enough anisotropy energy, the precise value of the overall energy scale g is irrelevant to the phase competition. There are four phases and four first-order phase transitions between them, occurring at high-symmetry points.

We now discuss the special case of graphene neutrality $\nu = 2$. At this filling factor there are exactly two filled Landau levels. In the fully symmetric $SU(4)$ limit one notes that a Slater determinant is an exact eigenstate :

$$|\Psi_{\nu=0}\rangle = \prod_m c_{m\alpha}^\dagger c_{m\beta}^\dagger |0\rangle, \quad (8)$$

where the orbital index m (whose precise definition is geometry dependent) takes all allowed values corresponding to complete integer filling, and α, β are two orthogonal vectors in four-dimensional spin-valley space spanned by $\{|K \uparrow\rangle, |K \downarrow\rangle, |K' \uparrow\rangle, |K' \downarrow\rangle\}$. Due to the $SU(4)$ symmetry these two vectors are arbitrary. The anisotropies will induce energy differences among all possibilities and determine the ground state spin-valley ordering. The mean-field treatment is performed by taking the expectation value of the anisotropy Hamiltonian Eq.(2) in the Slater determinant of Eq.(8). The result is given by a functional of the two vectors α and β :

$$\epsilon_a = \frac{1}{N_\phi} \langle \Psi_{\nu=0} | \mathcal{H}_{aniso} | \Psi_{\nu=0} \rangle = \sum_{i=x,y,z} u_i [tr(P_\alpha \tau_i) tr(P_\beta \tau_i) - tr(P_\alpha \tau_i P_\beta \tau_i)] \quad (9)$$

where we have defined the anisotropy energy per flux quantum ϵ_a , the projectors onto the trial vectors :

$$P_\alpha = |\alpha\rangle\langle\alpha|, P_\beta = |\beta\rangle\langle\beta|, \quad (10)$$

and the couplings are $u_x = u_y = u_\perp, u_z$. By minimization of this functional one finds four phases in the absence of Zeeman energy that are displayed in Fig.(1). There is a ferromagnetic phase (F) with $\alpha = |K \uparrow\rangle, \beta = |K' \uparrow\rangle$ which is stabilized in the range $-\pi/4 < \theta < +\pi/2$. One finds also an antiferromagnetic phase (AF) with $\alpha = |K \uparrow\rangle, \beta = |K' \downarrow\rangle$ preferred in the range $\pi/2 < \theta < 3\pi/4$. Note that this state is an antiferromagnet both in spin space and valley space. The Kékulé state (KD) has $\alpha = |\mathbf{n} \uparrow\rangle, \beta = |\mathbf{n} \downarrow\rangle$ where \mathbf{n} is a vector lying in the XY plane of the Bloch sphere for valley degrees of freedom : $\mathbf{n} = (|K\rangle + e^{i\phi}|K'\rangle)/\sqrt{2}$ where ϕ is an arbitrary angle in the valley XY plane. This state is a spin singlet but a XY valley ferromagnet. It is preferred in the range $3\pi/4 < \theta < 5\pi/4$. Finally the charge density wave state (CDW) defined by $\alpha = |K \uparrow\rangle, \beta = |K \downarrow\rangle$. This state is a spin singlet but a valley ferromagnet. Since the valley index coincides with the sublattice index in the central Landau level, this state has all the charge density on one sublattice and would be favored by a substrate breaking explicitly the sublattice symmetry like hexagonal boron nitride. It requires the range $5\pi/4 < \theta < 7\pi/4$ as it is stabilized by negative valley interactions along z direction.

All transitions between these various states are first-order within mean-field theory and this is confirmed by exact diagonalizations³⁹. Notably all transitions take place on the points with extra symmetries beyond the $U(1)$ valley

conservation. The spin quantum number of the ground state for a finite system as studied by exact diagonalization is given by $S = 0$ i.e. spin-singlet states for AF, KD and CDW phases while the F phase has maximal spin $S = N_e/2$. Concerning valley quantum numbers there are three phases with $T^z = 0$: F, AF, and KD while CDW has maximal valley polarization $T^z = N_e/2$.

With nonzero Zeeman energy the most notable change is that the AF phase becomes canted (CAF). The spins prefer to have antiparallel orientation in the plane perpendicular to the field direction and a small projection onto this direction. Increasing the Zeeman energy leads to greater ferromagnetic character and ultimately a phase transition from CAF to the F phase. The F phase has the very special characteristic of having conducting edge modes contrary to the CAF phase⁴⁵. The tilted-field experiments of ref.(11) enable the variation of the ratio of Zeeman vs. Coulomb energy scales. Since there is a metal-insulator transition in this set-up a natural explanation is that they observe the CAF-F transition. To be consistent with this scenario one deduces bounds on anisotropies :

$$u_{\perp} \simeq -10\epsilon_Z, \quad u_z + u_{\perp} > 0. \quad (11)$$

V. $SU(4)$ REPRESENTATIONS AND MODEL WAVEFUNCTIONS

In this section we describe how we use the theory of irreducible representations of the $SU(4)$ group in our exact diagonalization studies. Energy levels of a $SU(4)$ -invariant Hamiltonian are in general degenerate and form irreducible representations (irreps) of the symmetry group. These irreps are in one-to-one correspondence with Young tableaux that consist of three rows of boxes with L_1 boxes on the first row, L_2 boxes on the second row and L_3 on the third row with $L_1 \geq L_2 \geq L_3$. The dimension of such an irrep is given by :

$$\mathcal{D}(p_1, p_2, p_3) = \frac{1}{12}(p_1 + 1)(p_2 + 1)(p_3 + 1)(p_1 + p_2 + 2)(p_2 + p_3 + 2)(p_1 + p_2 + p_3 + 3), \quad (12)$$

where we have used the positive integers $p_1 = L_1 - L_2$, $p_2 = L_2 - L_3$, $p_3 = L_3$. It is also convenient to view such an irrep as a collection of irreps of $SU(2)$ subgroups that operate only on subsets of the basis states. We will use repeatedly the pure spin subgroup generated by $S^\alpha = \sigma^\alpha \otimes 1$ and the pure isospin subgroup generated by $T^\alpha = 1 \otimes \tau^\alpha$ acting on the valley degrees of freedom. They can be conveniently complemented by a third $SU(2)$ subgroup with generators $N^\alpha = \sigma^\alpha \otimes \tau^z$ that is inspired by Néel antiferromagnetic order. Although there are six independent such $SU(2)$ subgroups only these three are convenient because we will consider the additional symmetry-breaking perturbation given by Eq(2). A state belonging to a given $SU(4)$ irrep can be taken as an eigenstate of (S^z, T^z, N^z) simultaneously because these generators commute. Contrary to the simpler case of the $SU(2)$ group there is in general more than one state characterized by the three values (S^z, T^z, N^z) .

The $SU(4)$ symmetry implies that the second-quantized Hamiltonian of the Coulomb interaction preserves the number of particles of each species n_i with definite spin and valley so one may impose separately these numbers (n_1, n_2, n_3, n_4) and perform the diagonalization in the sector defined by these fixed numbers. The identification of an irrep is made by finding a highest weight state. This concept is familiar in the $SU(2)$ case. Indeed if one finds an energy value by imposing a given $S^z = M$ one does not know the total spin by this sole observation : we only know that the total spin of this level is larger than M . One has to find eigenenergies in sectors with $S^z = M + 1$ then $S^z = M + 2$ and so on up the point of disappearance of the energy level. The value of highest S^z containing a given energy is then equal to its *total* spin. A generalized reasoning applies in the $SU(4)$ case. If an energy eigenstate is found in some (n_1, n_2, n_3, n_4) sector one has to track it among states obtained by acting with raising operators till one finds a highest-weight state annihilated by all such operations. This is more computationally demanding than in the $SU(2)$ case. For a value of the highest weight $(S^z, T^z, N^z) = (m_1, m_2, m_3)$ the $SU(4)$ irrep is characterized by integers $p_1 = m_2 - m_3, p_2 = m_1 - m_2, p_3 = m_2 + m_3$ and the corresponding values of the lengths of Young tableau rows L_1, L_2, L_3 .

The picture that underlies our investigations is that eigenstates are essentially $SU(4)$ multiplets whose degeneracy is lifted only perturbatively by the anisotropies in Eq.(2). This is sensible as long as the anisotropy energies are not too large with respect to the Coulomb energy scale. Present experiments seem to be compatible with this point of view. It is important to note that the anisotropy energies are likely larger than the Zeeman energy in current experiments 11. All these symmetry considerations above are valid independently of the geometry we use. We make use of the spherical geometry⁴⁰ as well as of the torus geometry⁴⁶. The ground state of a FQHE system is expected to be uniform in space so on a sphere it should have zero total angular momentum and on the torus geometry where one can define magnetic many-body translations it should have also zero many-body momentum $K_x = K_y = 0$. While the pure Coulomb problem has the complete $SU(4)$ symmetry, the anisotropic case admit only spin T^z conservation. For practical reasons we implement only S^z and T^z conservation.

We now discuss trial wavefunctions that can be used to describe the fractional quantum Hall states with spin and valley degrees of freedom. We first make several remarks that apply to the $SU(4)$ symmetric limit. Note that any

$SU(2)$ Coulomb eigenstate is also an $SU(4)$ eigenstate. Only the degeneracy will change. If we have some $SU(2)$ Coulomb eigenstate constructed with two spin-valley vectors α and β and filling factor $\nu_{\alpha\beta}$ then we can glue a filled $\nu = 1$ complete Landau level for any vector γ and obtain another exact eigenstate of the Coulomb interaction with now filling factor $\nu = 1 + \nu_{\alpha\beta}$:

$$\Psi = \left\{ \prod_m c_{m\gamma}^\dagger \right\} \hat{\Psi}_{\alpha\beta}^\dagger |0\rangle, \quad (13)$$

where the operator $\hat{\Psi}_{\alpha\beta}^\dagger$ creates the $SU(2)$ state with two components. The energy of this new state is now given by :

$$E_{1+\nu_{\alpha\beta}} = E_1 + E_{\nu_{\alpha\beta}}, \quad E_1 = -\sqrt{\pi/8} E_C, \quad (14)$$

where E_1 is the energy of the completely filled level. In first-quantized language this gluing operation is the multiplication by the Vandermonde determinant of the $\nu = 1$ state. Note that this gluing operation also works if we use a single component state $\hat{\Psi}_\alpha$ instead of $\hat{\Psi}_{\alpha\beta}$.

In addition to the full particle-hole symmetry mapping ν to $4 - \nu$ one can also perform a particle-hole symmetry on only two flavours mapping (ν_1, ν_2) to $(1 - \nu_1, 1 - \nu_2)$ and the total filling is then transformed from ν to $2 - \nu$. Under this operation the energy becomes :

$$E_{2-\nu} = E_\nu + 2(1 - \nu)E_1. \quad (15)$$

These mappings Eqs(13,15) allow us to identify at least some of the eigenstates found by exact diagonalization. Of course there are also multicomponent states that cannot be generated from the 2-component case. Some of them have been found at filling factor $\nu = 2/3$ in a previous study⁴⁴. It is possible also to use these mappings to construct trial wavefunctions once we have a one or two-component state as obtained for example by the composite fermion construction^{47,48}. For the fractions we study, which are most prominent in experiments we cannot use known multicomponent generalizations^{49,50} of the Laughlin wavefunction because they lead to more complicated fractional fillings.

We adhere to the view that anisotropies are not strong enough to destroy the Coulomb correlations in a given trial state. It means that the small symmetry-breaking perturbations Eq.(2) will choose the orientation of the free vectors α, β, γ in a trial state like those of Eq.(13). Sodemann and MacDonald³⁸ have proposed an approximate scheme based on an extension of Hartree-Fock theory to estimate the anisotropy energy as a function of the free vectors in a trial state like Eq.(13). We note that it is fact feasible to compute directly the expectation value of the Hamiltonian for anisotropies in the trial states, bypassing any Hartree-Fock like approximation. Since the anisotropic interactions are purely point-like, the expectation value of the Hamiltonian Eq.(2) can be expressed in terms of the pair correlation function at the origin $g_{\alpha\beta}(0)$ generalizing the formula for $\nu = 2$:

$$\epsilon_a = \sum_{i=x,y,z} u_i \sum_{\alpha\beta} g_{\alpha\beta}(0) [tr(P_\alpha \tau_i) tr(P_\beta \tau_i) - tr(P_\alpha \tau_i P_\beta \tau_i)], \quad (16)$$

where the pair correlation function is that of the trial wavefunction. We define a more compact notation :

$$\epsilon_a = \sum_{\alpha\beta} g_{\alpha\beta}(0) \mathcal{F}_{\alpha\beta}, \quad (17)$$

where now the sum over α, β runs over all values involved in the trial wavefunction. The sum runs only over distinct values due to the Pauli principle ($g_{\alpha\alpha}(0) = 0$). If we consider trial states obtained by gluing a filled shell like in Eq.(13) then there are no non-trivial correlations between the completely filled shell and the other electrons : $g_{1\alpha}(0) = \nu_\alpha$. The case with two filled Landau levels $\nu_\alpha = \nu_\beta = 1$ gives the previous formula for the anisotropy energy Eq.(9). If we take a single-component state with filling ν_2 and glue a $\nu = 1$ shell then we obtain an energy which is simply the $\nu = 2$ formula multiplied by a ν_2 factor. Hence without any further calculation we can be sure that the phase diagram is identical to that of the $\nu = 2$ and is given in Fig.(1) with the same set of spin-valley vectors described above for the $\nu = 2$ case. However since the number of electrons is different in the two components, the quantum numbers of the ground state are different from those of the $\nu = 2$ case.

We now discuss the case with three occupied flavors with content $(1, \nu, \nu)$. The trial state is now a two-component state with flavor content (ν, ν) with a filled shell $\nu = 1$ glued onto it. The anisotropy energy is now given by :

$$\epsilon_a^{(1,\nu,\nu)} = \nu[\mathcal{F}_{\alpha\beta} + \mathcal{F}_{\alpha\gamma}] + g_{\beta\gamma}(0)\mathcal{F}_{\beta\gamma} \quad (18)$$

For the trial states we consider, the partially filled states will involve the two-component $\nu = 2/3$ and $\nu = 2/5$ spin-singlet states that have a very small pair correlation between different spin values $g_{\alpha\beta}(0) \approx 10^{-3}$. This very small number only slightly change the phase boundaries and can be safely discarded.

For matrix elements between two states $|\mathbf{t}_1\mathbf{s}_1\rangle, |\mathbf{t}_2\mathbf{s}_2\rangle$ (so without spin-valley entanglement) the matrix element \mathcal{F}_{12} is given by :

$$\mathcal{F}_{12} = \frac{1}{2}(1 - \mathbf{s}_1 \cdot \mathbf{s}_2) \left[\sum_i u_i t_{1i} t_{2i} \right] - \frac{1}{2}(1 + \mathbf{s}_1 \cdot \mathbf{s}_2) \frac{1}{2}(1 - \mathbf{t}_1 \cdot \mathbf{t}_2) \left[\sum_i u_i \right], \quad (19)$$

which allow us to obtain the variational energies for all cases of concern.

When discussing trial states we omit the unoccupied spin-valley states when displaying the component structure of the wavefunction i.e. $(1, 1/3, 0, 0)$ is written simply $(1, 1/3)$. However when describing an irrep we use all four components i.e. $(7, 4, 0, 0)$ stands for an $SU(4)$ irrep defined by its highest weight.

VI. FRACTIONS FOR $\nu < 1$

A. The $\nu = 1/3$ state

At filling factor $\nu = 1/3$ the one-component Coulomb ground state is an exact eigenstate of the $SU(4)$ symmetric case and it is a member of the irrep with highest weight $(N_e, 0, 0, 0)$. This means that the spatial part of the wave function is multiplied by a fully symmetrized wavefunction with all electrons in the same spin/valley state. The Zeeman field will orient the spin component and there will be a residual $SU(2)$ valley symmetry. Introduction of anisotropies Eq.(2) will have no effect on this eigenstate since the wavefunction exactly vanishes when two electrons coincides because of Pauli principle and the model anisotropies involve only contact interactions. In the real world there will be also further anisotropies involving relative angular momentum one and more that will act upon the eigenstate. However these effects can be estimated as being $O(a/\ell)$ smaller than the contact anisotropies. However it is worth mentioning that theoretical estimates of anisotropies are much smaller than the values required to explain the tilted-field transition between the F and CAF states at $\nu_G = 0$. So this means that presumably also the anisotropies involving relative angular momentum one and higher are not well known and may be larger than naive estimates so they could possibly be relevant even in the range of filling factor $\nu < 1$.

B. The $\nu = 2/3$ state

The situation is richer for $\nu = 2/3$. Several competing states are known to be present at this filling factor. First of all there is the one-component particle-hole symmetric of the $\nu = 1/3$ state which is again a one-component state. In the composite fermion description this fully polarized state has negative effective flux and composite fermions occupy two effective Λ -levels⁴⁸. With two components one can also construct a singlet state where now only one CF Λ level is occupied by singlet pairs. For pure Coulomb interactions the singlet state has lower energy than the polarized state by approximately $0.009E_C$ in the thermodynamic limit. These two states compete directly on the torus geometry while on the spherical geometry they have a different shift : the polarized state is realized for $N_\phi = (3/2)N_e$ and the singlet state for $N_\phi = (3/2)N_e - 1$.

While these two states are well-established in two-component FQHE systems, we note that there is evidence⁴⁴ for the formation of three-component and four-component states that are slightly lower in energy by $\approx 0.002E_C$. These enigmatic states are not easily explained by composite-fermion theory and finite size limitations lead to a large uncertainty in energy difference estimation. Such states are formed for $N_\phi = (3/2)N_e - 2$ on the sphere and they also appear on the torus geometry.

All these pure Coulomb eigenstates can be embedded in the four-component case giving rise to degenerate $SU(4)$ multiplets. Of course the $SU(4)$ singlet⁴⁴ observed for $N_e = 8$ is unaffected by anisotropies apart from a change in energy. The polarized $2/3$ state does not feel the delta function interactions of Eq.(2) but the singlet state has a nonvanishing probability of having two electrons at the same location provided they have different flavors : $g_{\alpha\neq\beta}(0) \neq 0$. This probability is small and is known to be of the order of 10^{-3} from exact diagonalization or CF wavefunctions. As a consequence the splitting induced by anisotropies is of order $g \times g_{\alpha\neq\beta}(0)$. If we use the variational approach of section (V) we obtain an energy functional which has exactly the same expression as in the $\nu = 2$ case apart from the overall scale. This means that the phase diagram is the one given in Fig.(1). We have checked by exact diagonalization that this phase diagram is correct beyond perturbation theory. Notably all characteristics of the phase transitions are unchanged between $\nu = 0$ and $\nu = 2/3$. The ground state quantum numbers of the finite system with $N = 6$ and $N_\phi = 8$ are consistent with the pattern of spin and valley ordering for $\nu = 2$.

VII. THE FRACTION $\nu = 4/3$

We now turn to the richer situation with fractions appearing for filling factors greater than one (and also less than two because of particle-hole symmetry). At the fraction $4/3$, by the remarks of section (V) we know that there are exact eigenstates in the $SU(4)$ symmetric limit obtained by adding a $\nu = 1$ shell to the $\nu = 1/3$ polarized eigenstate of the Coulomb problem. The flavor content of such a state is thus $(1, 1/3)$. There is also an eigenstate obtained by taking a $\nu = 2/3$ singlet involving only two flavors and making a particle-hole transformation on both flavors so that its final flavor content is $(2/3, 2/3)$. With the known properties of the particle-hole transformation Eq.(15) in fact we already know that the $(2/3, 2/3)$ state has lower Coulomb energy than $(1, 1/3)$ from the energies of the parent states in the thermodynamic limit. This remark was made in ref.(38). Beyond these two exact eigenstates it is not guaranteed that there are not intruders implying more components.

A. The $(1, 1/3)$ state

In the torus geometry there is no shift so these two states directly compete when we fix the flux and the number of particles, they differ only by the flavor partitioning. In this geometry the state $(1, 1/3)$ is an excited state and it is thus computationally demanding to study it.

In the sphere geometry for the first candidate $(1, 1/3)$ the total number of electrons is partitioned into two flavors $N_e = N_1 + N_2$ and N_1 electrons fully fill a spherical shell with flux N_ϕ while N_2 electrons form the usual $\nu = 1/3$ state :

$$N_\phi = N_1 - 1, \quad N_\phi = 3(N_2 - 1), \quad (20)$$

so that the flux-number of particles relationship is given by :

$$N_e = \frac{4}{3}N_\phi + 2, \quad (21)$$

Hence we can use the sphere geometry to study separately the two states $(1, 1/3)$ and $(2/3, 2/3)$. We have performed exact diagonalizations of the system with $N_e = 10$ and $N_\phi = 6$. While there is definitely a low-lying state with zero angular momentum $L = 0$ and irrep $(7, 3, 0, 0)$ as expected, it is not the ground state. Indeed the true ground state spans the irrep $(4, 4, 1, 1)$ with $L = 0$ and the irrep $(7, 3, 0, 0)$ is only the fourth excited state at this system size. At these rather small system sizes we consider that these states that lie below $(7, 3, 0, 0)$ are likely quasiparticle states with flavor changing excitations. The irrep $(7, 3, 0, 0)$ is split by the anisotropies as shown in Fig.(2). We have used a small value $\tilde{g} = 10^{-4}$ so that the states are not mixed with the nearby irreps. The low-lying states centered onto the parent symmetric state $(7, 3, 0, 0)$ are displayed in Fig.(2). There are four distinct phases separated by first-order transitions. The range of existence of these four phases is similar to the case for $\nu = 2$. However the quantum numbers we find are not always those predicted by the variational approach :

- For $-\pi/4 < \theta < +\pi/2$ there is a phase with $S = 5$ and $T^z = 2$ as expected for a ferromagnetic state. Since the two valleys should be populated by respectively seven and three electrons, one can have indeed the maximum possible spin $S = 5$ while T^z is given by the difference in valley occupation. However this is not the whole story since we observe that states with $T^z = 0, 1, 2$ are exactly degenerate while the full Hamiltonian does not have $SU(2)$ symmetry in the whole phase but only at the special point $\theta = \pi/4$. This is not predicted by the wavefunction in Eq.(8).
- For $+\pi/2 < \theta < +3\pi/4$ we find a phase with $S = 0$ and $T^z = 0$, which is natural to call antiferromagnetic. However it is definitely not in agreement with the variational quantum numbers ($S = 2$ and $T^z = 2$).
- For $+3\pi/4 < \theta < +5\pi/4$ the ground state has $S = 2$ and $T^z = 0$. The value of T^z points to XY valley order and these values are those predicted variationally. So we call this phase a Kékulé phase.
- Finally for $+5\pi/4 < \theta < +7\pi/4$ we find $S = 2$ and $T^z = 5$. The maximal value of T^z means that all electrons reside in a single valley i.e. a given sublattice as in a charge-density wave state and the total spin is correctly predicted by the variational wavefunction.

The most intriguing result is the appearance of exact valley multiplets when the state is completely polarized. This can be explained by the following line of reasoning : when we have full spin polarization the electrons occupy the two valleys and in the case of the $(1, 1/3)$ state one of these valleys is completely filled. If we perform a two-component

particle-hole transformation on the populated valleys we obtain a state $(0, 2/3)$ which is fully polarized since only one valley is occupied by holes. As a consequence there is no effect of anisotropies since they involve only a contact interaction, requiring space coincidence of electrons (as is the case of the $\nu = 1/3$ state discussed in section (VIA)). This does not imply that such states have energies independent of g_z, g_\perp parameters because they appear in the one-body terms in the particle-hole transformation. So there is a subset of states that do not feel degeneracy-lifting anisotropies when they are simply given by contact interactions. Note that this argument is also valid for excited states as long as they are also fully spin polarized

The total spin and valley polarizations certainly lead us to name these phases as F, AF, KD, CDW as in the $\nu = 2$ case. So the symmetry breaking pattern is the same as the neutrality case. However one of these four phases (AF) cannot be described by trial wavefunctions in Eq.(13) if we use for the spinors α and β the spinors that describe the $\nu = 2$ phase diagram. Another difference with respect to the neutrality case is that AF and KD phases do not have the same quantum numbers so the first-order transition between them involves a ground state level-crossing unlike the $\nu = 2$ case³⁹.

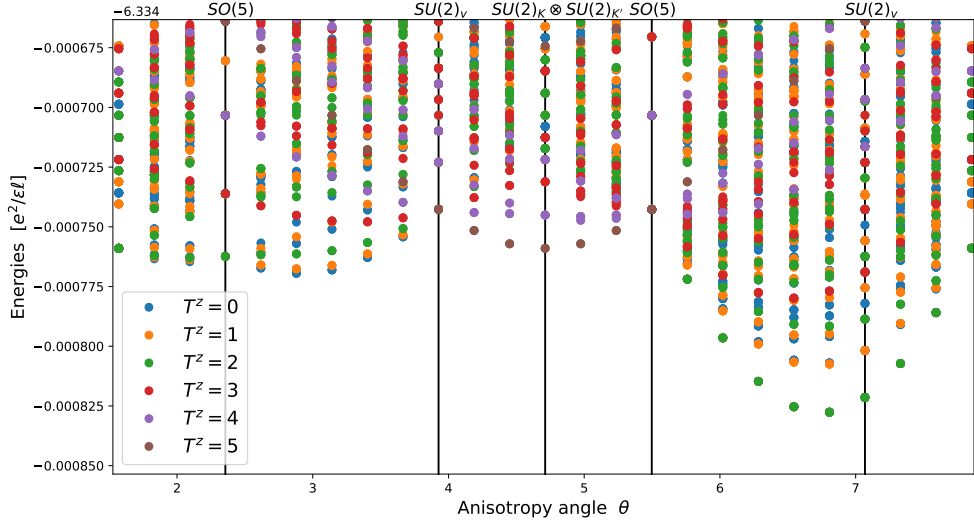


FIG. 2: Energy levels as a function of anisotropy for $\nu = 4/3$ on the sphere geometry with $N_e = 10$ and $N_\phi = 6$. The shift of the sphere geometry selects the $(1, 1/3)$ two occupied components of the highest-weight state. All these levels fan out from the parent unperturbed $SU(4)$ irrep which is $(7, 3, 0, 0)$. In the $SU(4)$ symmetric limit this irrep is not the ground state but it is the fourth excited state (fifth-lowest lying eigenstate). However it is the lowest-lying state with the expected quantum numbers for the $(1, 1/3)$ state. The vertical lines mark the special symmetry points of the anisotropic interaction model we use. We identify four different phases. They can be called F, AF, KD and CDW as in the neutral case with the caveat that the quantum numbers do not match those predicted by simple trial wavefunctions. Notably the AF phase is valley unpolarized and spin singlet. Also the ground state of the F phase is fully spin polarized as expected but form $SU(2)$ valley multiplets with $S = 5$ and $T = 2$. Unlike the $\nu = 2$ case, phases AF and KD no longer have the same quantum numbers and the phase transitions between them now involve a true level crossings at the $SO(5)$ point.

B. the $(2/3, 2/3)$ state

The well-known $SU(2)$ singlet state for $\nu = 2/3$ is obtained with a unit shift on the sphere geometry $N_\phi = (3/2)N_e - 1$ with $N_e = N_\uparrow + N_\downarrow$. If we make the particle-hole transformation $N_{\uparrow, \downarrow} \rightarrow N_\phi + 1 - N_{\uparrow, \downarrow}$ we obtain the relation $N_\phi = (3/4)N_e - 1$. When embedded in the 4-component space we expect to find an irrep with highest weight $(N_e/2, N_e/2, 0, 0)$ as the ground state. The degeneracy is then lifted by the anisotropy : in Fig.(3) we present results of exact diagonalizations in the sphere geometry for $N_e = 8$ electrons and $N_\phi = 5$. The important conclusion from this calculation is that the ground state quantum numbers are now exactly the same as in the $\nu = 2$ case. So the phase diagram is the same as in the $\nu = 2$ case : see Fig.(1) with the same behavior at the phase transition points. Notably the AF/KD phase transition has no ground state level crossing.

This is exactly what we find with the variational approach. Indeed with the particle-hole symmetric of the singlet state we have now $g_{\alpha\beta}(0)$ of order unity and an energy functional Eq.(16) equal to that of $\nu = 2$ except from an

overall factor.

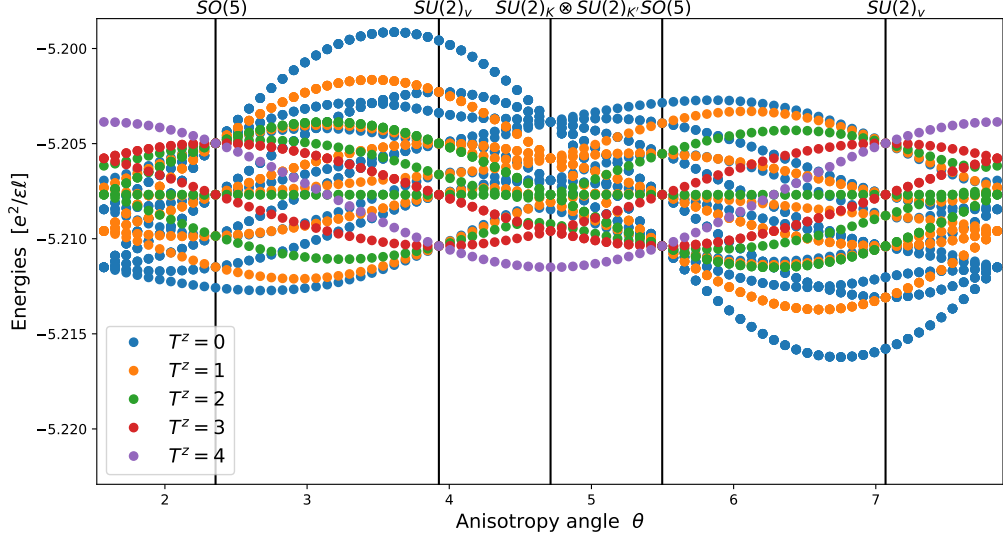


FIG. 3: Energy levels as a function of anisotropy for $\nu = 4/3$ on the sphere geometry with $N_e = 8$ and $N_\phi = 5$. The shift of the sphere geometry selects the $SU(2)$ two-component singlet $(2/3, 2/3)$ of the two occupied components of the highest-weight state. The parent unperturbed $SU(4)$ irrep is $(4, 4, 0, 0)$ which is the ground state in the symmetric limit. The vertical lines mark the special symmetry points of the anisotropic interaction model we use. We identify four different phases. The quantum numbers are exactly the same as in the neutrality case $\nu = 2$. We thus observe that the transition between AF and KD phases does not involve a ground state level crossing but presumably happens through the collapse of a tower of states.

While the $(2/3, 2/3)$ state is below the $(1, 1/3)$ state at zero Zeeman energy there may be a transition between these states that will be sensitive to the precise phase which is realized. This is discussed in section (IX).

VIII. THE FRACTION $\nu = 5/3$

Two possible candidates at this fraction are now $(1, 2/3)$ which is a two-component state and $(1, 1/3, 1/3)$ which is a genuine three-component state.

A. The two-component state $(1, 2/3)$

The first state is obtained by adding the polarized i.e. one-flavor $\nu = 2/3$ state to a filled level. This polarized state with $\nu = 2/3$ is the one-component particle-hole transform of the polarized Coulomb eigenstate at $\nu = 1/3$. The flux-number of particles is thus given by :

$$N_\phi = N_1 - 1, \quad N_\phi = 3/2 \times N_2, \quad N_e = N_1 + N_2, \\ N_\phi = \frac{3}{5}(N_e - 1).$$

We have performed sphere exact diagonalizations for $N_e = 11$ and $N_\phi = 6$. In the $SU(4)$ limit there is a lowest-lying state with $(7, 4, 0, 0)$ irrep and $L = 0$ as expected for the state obtained from the gluing procedure of Eq.(13) but it is not the ground state. This is the same phenomenon that we observe at $\nu = 4/3$. We posit that these extra states are flavor-changing quasiparticle excitations and focus only onto the fate of the $(7, 4, 0, 0)$ multiplet. By using a small value of the anisotropy $\tilde{g} = 10^{-4}$ the irrep is split in many levels but they do not mix with other multiplets. The result of this calculation is displayed in Fig.(4).

As in the case of the $(1, 1/3)$ state the quantum numbers are exactly those expected from using the spinors α and β describing the various orderings of $\nu = 2$ F, AF, KD, CDW and using them with Coulomb eigenstates in Eq.(13). Also since AF and KD do not have the same quantum numbers there is a level-crossing phase transition at the $SO(5)$ point between AF and KD phases.

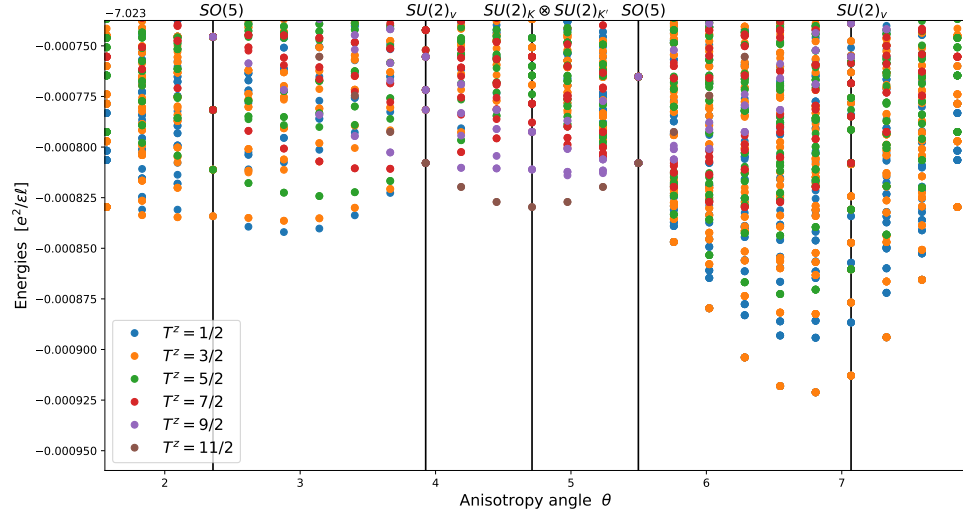


FIG. 4: Energy levels versus anisotropy angle θ for filling factor $\nu = 5/3$ on the sphere geometry with $N_e = 11$ and $N_\phi = 6$ selecting the $(1, 2/3)$ state. The parent $SU(4)$ irrep is $(7, 4, 0, 0)$. This state is not the absolute ground state in the $SU(4)$ limit: it is the sixth excited state. One finds four phases consistent with the $\nu = 2$ phase diagram but with distinct quantum numbers. There is a ferromagnetic phase for $-\pi/4 < \theta < +\pi/2$ with $S = 11/2$ and $T^z = 1/2, 3/2$ so there is an emergent $SU(2)$ valley symmetry, an antiferromagnetic phase for $+\pi/2 < \theta < +3\pi/4$ with $S = T^z = 3/2$, a Kékulé phase for $+3\pi/4 < \theta < +5\pi/4$ with $S = 3/2$ and $T^z = 1/2$ and a charge-density wave phase for $+5\pi/4 < \theta < +7\pi/4$ with $S = 3/2$ and $T^z = 11/2$. All transitions are first-order with level crossings.

In the fully polarized sector we observe also the appearance of degeneracies due to the $SU(2)$ valley symmetry not only at the special point $\theta = \pi/4$ but in the whole F phase. The manifold of $S = 11/2$ states involves indeed $T^z = 1/2$ and $T^z = 3/2$ while the variational prediction is that we should observe only $T^z = 3/2$. This is due to the same phenomenon we found for the ferromagnetic phase in the case of the $(1, 1/3)$ state. The two-component particle-hole symmetric state of the fully polarized states has valley content $(0, 1/3)$ so the holes being polarized do not feel the point-contact anisotropies.

B. the three-component state

For the three-component state one now replaces the $\nu = 2/3$ polarized state by the two-component singlet state at the same filling factor leading to a flavor content $(1, 1/3, 1/3)$. We call N_1 the number of electrons in the fully filled LL and N_2, N_3 the electron numbers in the two flavors forming the singlet state. We obtain thus a shift on the sphere which is different from that of the previous state :

$$N_\phi = N_1 - 1, \quad N_\phi = 3/2 \times (N_2 + N_3) - 1, \quad N_e = N_1 + N_2 + N_3, \\ N_\phi = \frac{3}{5}N_e - 1.$$

We have studied in detail the case $N_e = 10, N_\phi = 5$. In the $SU(4)$ limit we are already certain that this state is lower in energy than $(1, 2/3)$ since the $\nu = 2/3$ singlet is lower in energy than the polarized state at the same filling factor. We are also certain that there is such an eigenstate of the $SU(4)$ symmetric Coulomb problem.

The only remaining question is if there are some states lower in energy. Indeed it may very well be that by spreading the electrons into more flavors one can reduce the energy cost of Coulomb repulsion. If we consider the possible existence of an $SU(3)$ singlet state at filling $2/3$ with shift 2 on the sphere⁴⁴ then it implies the existence of a state with flavor content $(1, 2/9, 2/9, 2/9)$ and a flux given by $N_\phi = (3/5)N_e - (7/3)$. We observe on the sphere geometry that the ground state for $N_e = 14$ and $N_\phi = 7$ is spanned by the irrep $(8, 2, 2, 2)$. Since we already know⁴⁴ that there is a $SU(3)$ singlet $(2, 2, 2)$ for $N_e = 6$ and $N_\phi = 8$ this is in fact only a consistency check. Due to the severe size limitations of exact diagonalizations we cannot shed further light on this issue and limit ourselves to the states $(1, 2/3)$ and $(1, 1/3, 1/3)$. If there are states like $(1, 2/9, 2/9, 2/9)$ they are relevant only at small Zeeman energy.

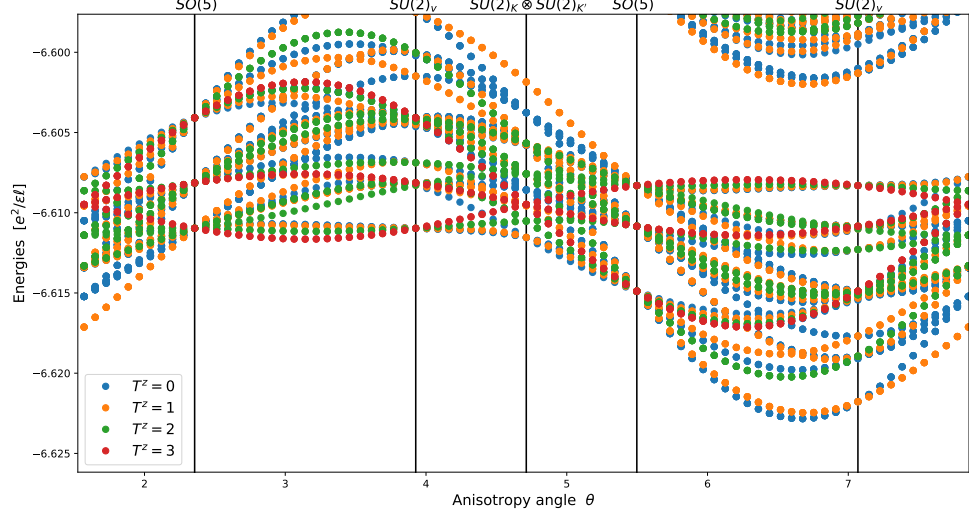


FIG. 5: Energy levels versus anisotropy angle θ for filling factor $\nu = 5/3$ on the sphere geometry with $N_e = 10$ and $N_\phi = 5$. This special shift favors the singlet state for the two partially occupied Landau levels so that the flavor content is $(1, 1/3, 1/3)$. The parent $SU(4)$ irrep is $(6, 2, 2, 0)$ and it is the ground state. The magnitude of the anisotropy is $\tilde{g} = 10^{-2}$. We observe five phases whose quantum numbers are displayed in Fig.(6). The five quantum phase transitions are first-order with true level crossings.

Our exact diagonalization results on the sphere geometry are presented in Fig.(5). We find now a phase diagram *different* from the neutrality case. There are five phase transitions and all of them involve level crossings in the finite systems. The five phases we observe have quantum numbers displayed in Fig.(6). Some of them may be captured by the variational approach but not all.

Since we are dealing with a three-component state it is no longer possible to have full spin or valley polarization. The maximal value of the spin is observed in the range $-\pi/4 < \theta < +3\pi/4$. In this regime we observe two phases A and B that differ by the valley T^z value.

- The A phase has no valley XY order and can be described by $\{\alpha, \beta, \gamma\} = \{|K \uparrow\rangle, |K' \uparrow\rangle, |K' \downarrow\rangle\}$ with $T^z = 1$ and $S = 3$.
- The B phase or $-\pi/4 < \theta < +\pi/4$ has $T^z = 0$ and is plausibly described by a state with $\{\alpha, \beta, \gamma\} = \{|\mathbf{t}_\perp \uparrow\rangle, |-\mathbf{t}_\perp \uparrow\rangle, |-\mathbf{t}_\perp \downarrow\rangle\}$. Due to the three-component nature of the state it is not possible to obtain $T^z = 0$ by using states with definite projections onto $|K\rangle, |K'\rangle$ but one has to use XY valley ordered states.

The transition between A and B phases is thus associated to the change of the valley order from Ising-type in A to XY-type in B .

The region $3\pi/4 < \theta < 3\pi/2$ has now only partial spin polarization and is divided into two phases that differ by a change in the value of the valley polarization.

- We find a phase E_1 for $3\pi/4 < \theta < 5\pi/4$ with the maximal value of T^z . $\{\alpha, \beta, \gamma\} = \{|K \uparrow\rangle, |K \downarrow\rangle, |K' \downarrow\rangle\}$
- In the lower quadrant $5\pi/4 < \theta < 3\pi/2$ we have a phase E_2 with $T^z = 0$ indicative of XY valley ordering whose candidate ordering pattern is given by $\{\alpha, \beta, \gamma\} = \{|\mathbf{t}_\perp \uparrow\rangle, |-\mathbf{t}_\perp \downarrow\rangle, |\mathbf{t}_\perp \downarrow\rangle\}$. The transition between E_1 and E_2 corresponds in changing the valley order from the Ising-like z -axis to the valley XY plane. A variational treatment does not distinguish between Ising or XY character in this range of anisotropies. Indeed all states are degenerate with trial energy in Eq.(16).
- Finally there is a fifth phase that we call C for $3\pi/2 < \theta < 7\pi/4$ which is a spin singlet $S = 0$ as well as valley unpolarized $T^z = 0$. It is not possible to capture such a phase with the class of variational states discussed above. If we look at the full set of degenerate states in the $SU(4)$ limit, one notes that the irrep $(6, 2, 2, 0)$ that we study contains notably symmetric states like $(3, 2, 2, 3)$ from which one can construct states with zero spin and zero isospin values. It is an open question to obtain explicitly a wavefunction with the correct quantum numbers for the C phase.

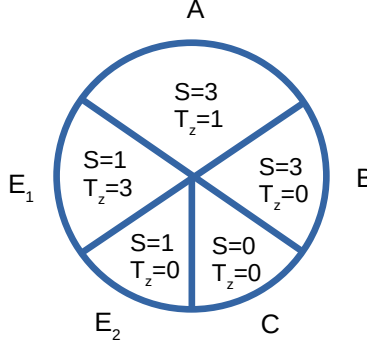


FIG. 6: Phase diagram for the $\nu = 5/3$ with $N_e = 10$ and $N_\phi = 5$. The parent $SU(4)$ irrep is $(6, 2, 2, 0)$. This is valid on the sphere geometry. On the torus geometry the quantum numbers are slightly different since the number of states per Landau level differ by one unit. While A, B can be captured plausibly by the variational method, it is not case of the singlet phase C . The $E_{1,2}$ phase are found to be degenerate variationally while our results show that they differ by type of valley ordering.

To shed some more light onto the nature of the C phase we have computed the pair correlation function $g_{\alpha\beta}(r)$ of the exact ground state in the sphere geometry. With a ground state having zero spin and $T^z = 0$ there are only four independent combinations of spin-valley that are plotted in Fig.(7). At short distance the leading correlation is $g_{K\uparrow K\downarrow}(0) = g_{K'\uparrow K'\downarrow}(0)$. This function has a maximum at the origin while all other cases have a deep minimum as expected from Coulomb repulsion. This may point to formation of spin $S=0$ singlet pairs in each valley. On the contrary the antiferromagnetic-like repulsion between $K\uparrow$ and $K'\downarrow$ is maximal at a finite distance $\approx 2.5\ell$.

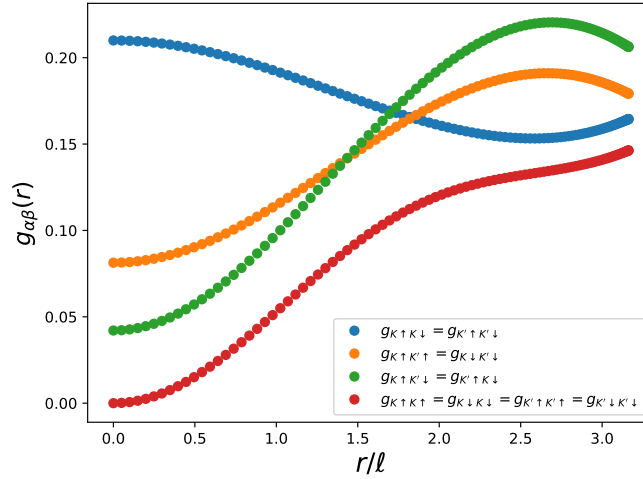


FIG. 7: The various pair correlation functions $g_{\alpha\beta}(r)$ calculated in the middle of the singlet C phase for $\theta = 3\pi/2 + \pi/8$. The sphere geometry is used with $N_e = 10, N_\phi = 5$. The chord distance r varies from zero up to $\sqrt{10}\ell$. Since we have $S^z = 0$ and $T^z = 0$ in this phase there are only four distinct correlations.

IX. SPIN TRANSITIONS

In the case of filling factor $\nu = 2/3$ it is well known⁴² that one can induce a spin transition between the singlet state and the fully polarized state. Indeed while the polarized state has a higher Coulomb energy, increasing the Zeeman energy will lower it eventually below the singlet state. The crossing happens when the Zeeman energy equals the energy difference between the two states :

$$\Delta E = \epsilon_Z B_{crit}. \quad (22)$$

This prototypical transition is simple because of the well-defined magnetization of the two competing states. Here in monolayer graphene the situation is richer since the competing states that we have studied above can have various magnetizations according to the value of the anisotropy parameters. The Coulomb energy scales as $\propto \sqrt{B}$ while anisotropy energies and the Zeeman energy scale linearly with B . The energy per particle of a state i has thus three contributions :

$$\epsilon_i = E_{Ci} + a_i B + \epsilon_Z m, \quad (23)$$

where we have defined the magnetization per particle m and the Coulomb energy E_{Ci} . A spin transition between two states 0 and 1 arises when the Coulomb energy difference is equal to the contribution from anisotropies and Zeeman energy :

$$\Delta\epsilon_{01}(B_{crit}) = (a_0 - a_1 + z)B_{crit} \quad (24)$$

The Zeeman factor z depends upon the magnetization of the two competing states and in the case of monolayer graphene it takes different values in different parts of anisotropy phase diagram.

We now give a simplified description of spin transitions for the fractions we have studied. We limit ourselves to situations with only a perpendicular field and also we ignore the possibility of spin canting. Indeed the effect of the canting is restricted to low enough fields. At large enough values of the field one obtains a fully polarized state or a collinear antiferromagnet depending on the filling fraction. Certainly spin canting may drive interesting transitions but detailed predictions are hampered by our lack of knowledge about the values of anisotropies.

A. $\nu = 2/3$

At filling factor $2/3$ the polarized state is insensitive to anisotropies while the singlet state can be in any of four phases F, AF, CDW, KD as shown in section (VIB). In KD or CDW the state is a spin singlet so it is insensitive to the Zeeman coupling. We thus expect a spin transition towards the fully polarized state at some field value Eq.(24). The AF state turns into a canted antiferromagnetic state which becomes fully polarized beyond some field value. Once in this fully polarized state, as is the case of the F phase, the state lowers its energy at the same rate as the polarized $\nu = 2/3$ state so that there will be no crossing hence there will be no spin transition in the AF or F phases.

B. $\nu = 4/3$

The phase diagrams for the states $(1, 1/3)$ and $(2/3, 2/3)$ are similar : there is the same number of phases with their domain of stability having the same range of anisotropy angle θ . but the difference is now in their total magnetization. In the F phase the two states have the same total spin value so they never cross under Zeeman coupling. In the KD and CDW phases the situation is different. In the state $(2/3, 2/3)$ there is zero net magnetization in both cases KD and CDW while in the state $(1, 1/3)$ the KD phase has now a net magnetization equal to $1/3$ of the saturation value and the CDW phase has an even smaller magnetization (but nonzero). So we deduce that there can be a spin transition in both phases KD and CDW.

C. $\nu = 5/3$

The situation is more complex since now the phase diagrams of the two competing states $(1, 2/3)$ and $(1, 1/3, 1/3)$ do not overlap exactly as a function of anisotropy. We describe the situation by using as a reference the phases of the $(1, 2/3)$ state. In the F phase the state $(1, 2/3)$ is fully polarized with magnetization $M = M_{sat}$ while A and B phases of $(1, 1/3, 1/3)$ have only $M = M_{sat}/\nu$ so we expect a spin transition. In KD and CDW phases the higher-lying state $(1, 2/3)$ has $M = M_{sat}/3$ while the competing phases in $(1, 1/3, 1/3)$ are the C and E_2 phases (see Fig.(6)). In the singlet C phase we have $M = 0$ and in the E_1 and E_2 phases $M = M_{sat}/5$ so there will be a spin transition. Its location B_{crit} will be phase dependent because there are (yet unknown) contributions from anisotropies in the value of the critical field in Eq.(24).

The general picture is that states with maximal spread-out of electrons in various spin-valley components will be favored only at small Zeeman energies. Notably graphene experiments with large Zeeman splittings and large sublattice effects like measurements in ref.(20) will involve only states like $(1, 1/3)$ and $(1, 2/3)$ as well as their generalizations to other fractions. Genuine multicomponent states will require minimal effect of the one-body fields.

X. CONCLUSION

We have studied the impact of anisotropies relevant to the description of monolayer graphene in the regime of the fractional quantum Hall effect. At neutrality the phase diagram involves four phases F, AF, KD and CDW. Simple generalizations of this diagram apply for $\nu = (1/3, 1/3)$, $\nu = (2/3, 2/3)$ and $\nu = (1, 2/3)$ states. This is found from exact diagonalizations on the sphere geometry and is also confirmed by a variational approach involving parent Coulomb eigenstates. The two spin-valley vectors α, β that characterize the spin-valley order in the variational approach are identical to the neutral case. Since the occupations of the two filled states are in general not equal it means that the quantum numbers of the ground state are now different from the neutral case. As a consequence all first-order transitions involve level crossings. Indeed there is no evidence for exotic phase transitions⁵¹.

In the case of $\nu = (1, 1/3)$ there are also four phases whose range of stability is the same as the neutral case but the quantum numbers are not all predicted by the variational method. While CDW and KD-like phases have spin and valley quantum numbers correctly predicted, we find that the antiferromagnetic phase is a spin singlet with no net valley polarization. Interestingly we find that the fully polarized states partly escape effects of anisotropy and still form $SU(2)$ valley multiplets even though this is not a symmetry of the Hamiltonian (their energies still depend upon g_z and g_\perp). This emergent symmetry also appears in the polarized eigenstates of the $(1, 2/3)$ state.

The case $\nu = (1, 1/3, 1/3)$ is different. We observe five phases. Two of them can be described variationally. There are two distinct phases in our diagonalizations that differ by Ising valley order versus XY valley order while they are degenerate variationally. There is also a phase which a spin singlet with presumably XY valley order that happens for negative Ising-like anisotropy. It is an open question how to write a wavefunction to describe this phase. The pair correlation function $g_{\alpha\beta}(0)$ shows an enhanced probability for electrons for opposite spins but in the same valley to be at the same location. This interesting situation requires however low Zeeman energy to be realized experimentally.

In present experiments it is likely that one observes the two-component states $(1, 1/3)$ and $(1, 2/3)$. If they are fully polarized (the F phase) then we predict that they should escape degeneracy-lifting anisotropies of the form given in Eq.(2) and thus feature an emergent valley $SU(2)$ symmetry. Invalidating this valley symmetry would invalidate the simplified model of Eq.(2) which is a crucial piece of our present understanding of IQHE and FQHE in graphene systems.

Recent experiments using scanning tunneling microscopy^{52,53} have given evidence for a more complex picture at neutrality $\nu = 0$ than previously thought. Notably there is evidence for phases beyond the four states of Fig.(1). There are at least two possible explanations. It may very well be that the anisotropies are not small in comparison to coulomb and that the simple model Eq.(2) is not adequate. It may also mean that the Landau level mixing is strong enough to change the phase structure. Such a possibility would invalidate standard theoretical treatments that focus on a fixed Landau level from the start. Also some of the experiments⁵² favor a Kékulé state which is at odds with the explanation of the metal-insulator transition¹¹. This may mean that the anisotropy parameters are not in the range of Eq.(11) in which case the explanation for the tilted-field transition becomes more elusive. It may be that the edge of the sample lies in a different phase from the bulk as observed in Hartree-Fock studies⁵⁴.

Acknowledgments

We acknowledge discussions with A. Assouline and P. Roulleau. We thank C. Repellin for useful correspondence. We thank DRF and GENCI-CCRT for computer time allocation on the Cobalt and Topaze clusters.

-
- ¹ D. C. Tsui, H. L. Stormer, and A. C. Gossard, Phys. Rev. Lett. **48**, 1559 (1982).
 - ² C. Nayak, S. H. Simon, A. Stern, M. Freedman, and S. Das Sarma, Rev. Mod. Phys. **80**, 1083 (2008).
 - ³ J. Eisenstein and A. H. MacDonald, Nature (London) **432**, 691 (2004).
 - ⁴ S. L. Sondhi, A. Karlhede, S. A. Kivelson, and E. H. Rezayi, Phys. Rev. B **47**, 16419 (1993).
 - ⁵ K. Moon, H. Mori, K. Yang, S. M. Girvin, A. H. MacDonald, L. Zheng, D. Yoshioka, and S.-C. Zhang, Phys. Rev. B **51**, 5138 (1995).
 - ⁶ E. P. De Poortere, Y. P. Shkolnikov, E. Tutuc, S. J. Papadakis, M. Shayegan, E. Palm, and T. Murphy, Appl. Phys. Lett. **80**, 1583 (2002).
 - ⁷ X. Du, I. Skachko, F. Duerr, A. Luican, and E. Y. Andrei, Nature **462**, 192 (2009).
 - ⁸ K. I. Bolotin, F. Ghahari, M. D. Shulman, and H. L. Stormer, P. Kim, Nature **462**, 196 (2009).
 - ⁹ F. Ghahari, Y. Zhao, P. Cadden-Zimansky, and K. Bolotin, P. Kim, Phys. Rev. Lett. **106**, 046801 (2011).
 - ¹⁰ C. R. Dean, A. F. Young, P. Cadden-Zimansky, L. Wang, H. Ren, K. Watanabe, T. Taniguchi, P. Kim, J. Hone, and K. L. Shepard, Nature Physics **7**, 693 (2011).

- ¹¹ A. F. Young, C. R. Dean, L. Wang, H. Ren, P. Cadden-Zimansky, K. Watanabe, T. Taniguchi, J. Hone, K. L. Shepard, and P. Kim, *Nature Phys.* **8**, 550 (2012).
- ¹² B. E. Feldman, B. Krauss, J. H. Smet, and A. Yacoby, *Science* **337**, 1196 (2012).
- ¹³ B. E. Feldman, A. J. Levin, B. Krauss, D. A. Abanin, B. I. Halperin, J. H. Smet, and A. Yacoby, *Phys. Rev. Lett.* **111**, 076802 (2013).
- ¹⁴ B. Hunt, J. D. Sanchez-Yamagishi, A. F. Young, M. Yankowitz, B. J. LeRoy, K. Watanabe, T. Taniguchi, P. Moon, M. Koshino, P. Jarillo-Herrero, and R. C. Ashoori, *Science* **340**, 1427 (2013).
- ¹⁵ A. F. Young, J. D. Sanchez-Yamagishi, B. Hunt, S. H. Choi, K. Watanabe, T. Taniguchi, R. C. Ashoori, and P. Jarillo-Herrero, *Nature* **505**, 528 (2014).
- ¹⁶ F. Amet, A. J. Bestwick, J. R. Williams, L. Balicas, K. Watanabe, T. Taniguchi, and D. Goldhaber-Gordon, *Nature Commun.* **6**:5838 (2015).
- ¹⁷ A. A. Zibrov, E. M. Spanton, H. Zhou, C. Kometter, T. Taniguchi, K. Watanabe, and A. F. Young, *Nature Physics*, **14**, 930 (2018).
- ¹⁸ H. Polshyn, H. Zhou, E. M. Spanton, T. Taniguchi, K. Watanabe, and A. F. Young, *Phys. Rev. Lett.* **121**, 226801 (2018).
- ¹⁹ S. Chen, R. Ribeiro-Palau, K. Yang, K. Watanabe, T. Taniguchi, J. Hone, M. O. Goerbig, and C. R. Dean, *Phys. Rev. Lett.* **122**, 026802 (2019).
- ²⁰ Y. Zeng, J. I. A. Li, S. A. Dietrich, O. M. Ghosh, K. Watanabe, T. Taniguchi, J. Hone, and C. R. Dean, *Phys. Rev. Lett.* **122**, 137701 (2019).
- ²¹ H. Zhou, H. Polshyn, T. Taniguchi, K. Watanabe, and A. F. Young, *Nature Physics* **16**, 154 (2020).
- ²² F. Yang, A. A. Zibrov, R. Bai, T. Taniguchi, K. Watanabe, M. P. Zaletel, and A. F. Young, *Phys. Rev. Lett.* **126**, 156802 (2021).
- ²³ H. Zhou, C. Huang, N. Wei, T. Taniguchi, K. Watanabe, M. P. Zaletel, Z. Papic, A. H. MacDonald, and A. F. Young, “Strong-Magnetic-Field Magnon Transport in Monolayer Graphene”, e-print arXiv:2102.01061.
- ²⁴ K. Yang, S. DasSarma, and A. H. MacDonald, *Phys. Rev. B* **74**, 075423 (2006).
- ²⁵ J. Jung and A. H. MacDonald, *Phys. Rev. B* **80**, 235417 (2009).
- ²⁶ M. Kharitonov, *Phys. Rev. B* **85**, 155439 (2012); *Phys. Rev. B* **86**, 075450 (2012).
- ²⁷ V. M. Apalkov and T. Chakraborty, *Phys. Rev. Lett.* **97**, 126801 (2006).
- ²⁸ C. Töke, P. E. Lammert, V. H. Crespi, and J. K. Jain, *Phys. Rev. B* **74**, 235417 (2006).
- ²⁹ C. Töke and J. K. Jain, *Phys. Rev. B* **75**, 245440 (2007).
- ³⁰ N. Shibata and K. Nomura, *Phys. Rev. B* **77**, 235426 (2008).
- ³¹ N. Shibata and K. Nomura, *J. Phys. Soc. Jpn* **78**, 104708 (2009).
- ³² C. Töke and J. K. Jain, *J. Phys.: Condens. Matter* **24**, 235601 (2012).
- ³³ Z. Papic, M. O. Goerbig, and N. Regnault, *Phys. Rev. Lett.* **105**, 176802 (2010).
- ³⁴ A. C. Balram, C. Töke, A. Wójs, and J. K. Jain, *Phys. Rev. B* **92**, 205120 (2015).
- ³⁵ A. C. Balram, C. Töke, A. Wójs, and J. K. Jain, *Phys. Rev. B* **92**, 075410 (2015).
- ³⁶ A. C. Balram, C. Töke, A. Wójs, and J. K. Jain, *Phys. Rev. B* **91**, 045109 (2015).
- ³⁷ D. A. Abanin, B. E. Feldman, A. Yacoby, and B. I. Halperin, *Phys. Rev. B* **88**, 115407 (2013).
- ³⁸ I. Sodemann and A. H. MacDonald, *Phys. Rev. Lett.* **112**, 126804 (2014).
- ³⁹ F. C. Wu, I. Sodemann, Y. Araki, A. H. MacDonald, and Th. Jolicoeur, *Phys. Rev. B* **90**, 235432 (2014).
- ⁴⁰ F. D. M. Haldane, *Phys. Rev. Lett.* **51**, 605 (1983); F. D. M. Haldane, in *The Quantum Hall Effect*, edited by R. Prange and S. Girvin (Springer-Verlag New York, 1987), Vol. 1, Chap. 8.
- ⁴¹ G. Fano, F. Ortolani, and E. Colombo, *Phys. Rev. B* **34**, 2670 (1986).
- ⁴² H. M. Yoo, K. W. Baldwin, K. West, L. Pfeiffer, and R. C. Ashoori, *Nat. Phys.* **16**, 1022 (2020).
- ⁴³ J. Alicea and M. P. A. Fisher, *Phys. Rev. B* **74**, 075422 (2006).
- ⁴⁴ F. C. Wu, I. Sodemann, A. H. MacDonald, and Th. Jolicoeur, *Phys. Rev. Lett.* **115**, 166805 (2015).
- ⁴⁵ D. A. Abanin, P. A. Lee, and L. S. Levitov, *Phys. Rev. Lett.* **96**, 176803 (2006).
- ⁴⁶ E. H. Rezayi, and F. D. M. Haldane, *Phys. Rev. B* **32**, 6924 (1985).
- ⁴⁷ J. K. Jain, *Phys. Rev. Lett.* **63**, 199 (1989).
- ⁴⁸ J. K. Jain. *Composite fermions*. Cambridge University Press, Cambridge UK (2007).
- ⁴⁹ B. I. Halperin, *Helv. Phys. Acta* **56**, 75 (1983).
- ⁵⁰ A. H. MacDonald, *Surface Science*, **229**, 1 (1990).
- ⁵¹ J. Lee and S. Sachdev, *Phys. Rev. Lett.* **114**, 226801 (2015).
- ⁵² X. Liu, G. Farahi, C.-L. Chiu, Z. Papic, K. Watanabe, T. Taniguchi, M. P. Zaletel, and A. Yazdani, “Visualizing Broken Symmetry and Topological Defects in a Quantum Hall Ferromagnet”, eprint arXiv 2109.11555.
- ⁵³ A. Coissard, D. Wander, H. Vignaud, A. G. Grushin, C. Repellin, K. Watanabe, T. Taniguchi, F. Gay, C. Winkelmann, H. Courtois, H. Sellier, and B. Sacépé, “Imaging tunable quantum Hall broken-symmetry orders in charge-neutral graphene”, eprint arXiv 2110.02811.
- ⁵⁴ A. Knothe and Th. Jolicoeur, *Phys. Rev. B* **92**, 165110 (2015).